

Electron spin resonance and microwave absorption study of MgB_2

V. Likodimos and M. Pissas

Institute of Materials Science, NCSR, Demokritos, 153 10 Aghia Paraskevi, Athens, Greece

(Received 11 September 2001; revised manuscript received 1 March 2002; published 25 April 2002)

A comparative study of powder and bulk specimens of MgB_2 by electron spin resonance (ESR) verifies the presence of intense conduction electron spin resonance (CESR) in the normal state. A low concentration paramagnetic center stemming from the initial amorphous boron powder along with traces of Fe^{3+} impurities are identified in the ESR spectra. Intense microwave absorption, that distorts CESR below T_c , is observed in fine powders implying enhanced microwave dissipation due to the viscous flux motion.

DOI: 10.1103/PhysRevB.65.172507

PACS number(s): 74.70.Ad, 76.30.Pk, 74.25.Nf, 74.60.Ge

The recent discovery of superconductivity in magnesium diboride (MgB_2), with $T_c \approx 39$ K,¹ has been the stimulus for intensive studies (for a recent review see Ref. 2 and references therein) aimed at a firm understanding of its fundamental properties and their implications on the application potential of MgB_2 driven by the high critical current densities J_c , sustained in polycrystalline materials.³

Electron-spin resonance (ESR) is known to be a very sensitive method to probe paramagnetic centers and microwave absorption in both conventional and high- T_c superconductors.⁴ Recently, a thorough ESR study revealed conduction-electron spin resonance (CESR) in fine powders of MgB_2 , both in normal and superconducting state at fields well below the upper critical field H_{c2} for MgB_2 ,⁵ that is classified as a type-II superconductor with $H_{c2}^{ab}(0) \approx 160$ kOe.⁶ An anisotropy ratio $\gamma = H_{c2}^{ab}/H_{c2}^c \approx 6-9$ was deduced from the splitting of CESR at high fields, in accord with the magnetization analysis of random powders ($\gamma \approx 6$) (Ref. 7) and a recent NMR and magnetization study.⁸

In this work, we report X-band ESR measurements on polycrystalline MgB_2 in powder and bulk form, revealing the intense CESR in the normal state. A paramagnetic center of low concentration along with traces of Fe^{3+} impurities are also observed. CESR is distorted below T_c by intense modulated microwave absorption dominated by viscous fluxon motion rather than the weak-link induced dissipation amply identified in high- T_c superconductors.

Polycrystalline MgB_2 was synthesized by direct reaction of Mg and amorphous B powders, as described in Ref. 9. X-ray powder diffraction refinement showed single-phase materials with a small amount ($\approx 2.5\%$) of MgO .⁹ ac susceptibility revealed a sharp ($\Delta T \approx 0.8$ K) superconducting transition with $T_c = 38.6$ K for both bulk pieces and fine powders. However, isothermal magnetization measurements showed a pronounced change from symmetric to asymmetric hysteresis loops, implying an intriguing crossover from bulk to surface pinning, when bulk pieces were ground into fine powders.⁹

ESR measurements were performed on an X-band Bruker 200D spectrometer ($\nu \approx 9.42$ GHz) with a rectangular TE102 mode resonant cavity and a 100-kHz field modulation. The modulation amplitude was kept constant at $4G_{pp}$ in the ESR spectra reported hereafter. The magnetic field was scaled with a NMR gaussmeter, while temperature-

dependent measurements were carried out employing an Oxford flow cryostat. The g factor and the ESR intensity were calibrated using standard samples of diphenyl-picrylhydrazyl ($g = 2.0036$), weak coal pitch ($g = 2.0028$) and $\text{CuSO}_4 \cdot 5\text{H}_2\text{O}$. Measurements were performed in both bulk pieces and fine powders obtained after thorough grinding. In some cases, the fine MgB_2 powder was further mixed with ESR silent SnO_2 to ensure good separation of the grains.

Figure 1 shows representative ESR spectra of a finely ground MgB_2 specimen at various temperatures. For comparison, the ESR spectrum of a bulk MgB_2 piece is shown at room temperature (RT). All spectra were recorded under the same conditions for samples of the same batch with approximately equal mass ($m \approx 4$ mg). A CESR signal is clearly observed, with an asymmetric metallic line shape indicated by the different amplitude of the maximum (A) and minimum (B) of the derivative of the absorbed power (Fig. 1). The CESR intensity is substantially decreased, approximately by an order of magnitude, in the bulk specimen, in accord with the reduced penetration of the microwave field due to the skin effect. The asymmetric CESR line can be adequately simulated by a linear superposition of the deriva-

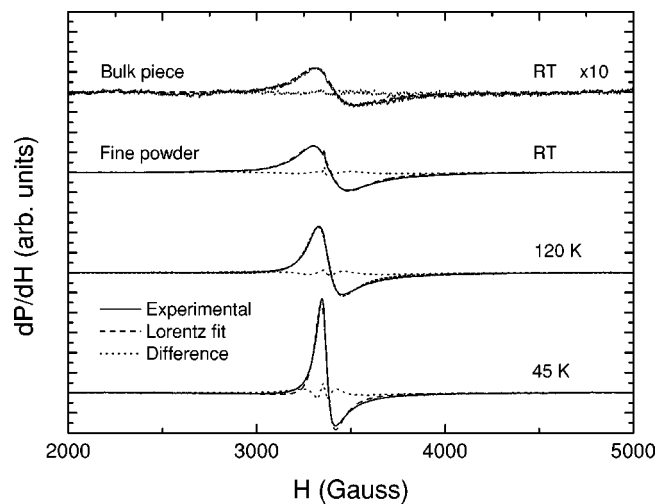


FIG. 1. Temperature dependence of CESR for a fine powder MgB_2 specimen at 9.4 GHz. The spectrum of a bulk piece is shown for comparison at RT. The best-fit Lorentzian line shape and the difference from the experimental CESR line are shown by dashed and dotted lines, respectively.

tives of the absorptive and dispersive parts of a Lorentzian line (Fig. 1), implying a homogeneous line broadening, consistent with finely ground metallic specimens with a skin depth δ comparable to the sample thickness θ .¹⁰ The asymmetry ratio A/B increases from about 1.5 at RT to 2.8 at 45 K, indicating a dominant contribution from grains with $\theta/\delta \sim 1.0$ and 1.7, respectively. At lower T , the CESR intensity decreases as the size of the grains becomes comparable to or even larger than the skin depth, which was estimated for MgB_2 at 9 GHz to be $\delta \approx 1.6 \mu\text{m}$ at 300 K and $\delta \approx 0.3 \mu\text{m}$ at 40 K, yielding a reduction of the intensity by $\sim 25\%$. The apparent A/B ratio for the bulk specimen at RT is close to 2.0 differing from the lower limiting value of ~ 2.5 expected for homogeneous thick samples and stationary spins,¹¹ probably due to the irregular morphology and connectivity of surface grains. Accordingly, a major contribution of crystallites most likely located near the surface with $\theta/\delta \sim 1.3$ and $\theta \sim 2.1 \mu\text{m}$, might be inferred.

The g factor determined from the Lorentz fit of the CESR line increases slightly from $g = 1.998(1)$ at RT to $g = 2.0015(5)$ at 45 K, in agreement with the CESR study of MgB_2 , showing a small deviation from the free-electron g value.⁵ The CESR intensity determined from several MgB_2 powder samples at RT, after being corrected for the skin effect,¹² corresponds to a spin susceptibility of $\chi_s = 2.5(4) \times 10^{-5}$ emu/mole, which leads to a density of states at the Fermi energy of about 0.77(12) states/eV. This value is in reasonable agreement with the CESR results⁵ and band-structure calculations.¹³ The resonance width ΔH (half-width at half-height) narrows continuously from $\Delta H = 163(1)$ G at RT to 62(1) G at 45 K, in accord with the decreasing behavior of the normal resistance as T decreases. However, the observed ΔH values are larger, approximately by 60 G at RT and 40 G at 45 K, than the CESR widths reported for MgB_2 ,⁵ implying an increased contribution from impurity and/or surface scattering.

Decomposition of the CESR signal reveals an additional, narrow ESR line with $g = 2.0026(5)$ and $\Delta H \approx 10(1)$ G at RT, already traced by the small peak superimposed on the center of the ESR spectra (Fig. 1). The weak intensity of this ESR line, whose presence was verified in all samples of the same batch, yields a spin concentration of roughly $\sim 5 \times 10^{17}$ spin/g, corresponding to a low Curie constant of $C \sim 1.3 \times 10^{-5}$ emu K/mole at RT. The narrow ESR line, probed by the Lorentzian fit (Fig. 1), persists down to the lowest T in the normal state with $g = 2.004(1)$ and a broader width $\Delta H_{pp} = 20(3)$ G. Its intensity is reduced compared to the paramagnetic $\sim 1/T$ variation by the same amount as the CESR signal, implying a dominant contribution of the skin effect. Traces of Fe^{3+} impurities were also detected in a temperature range of 40–60 K through the observation of a typical $g = 4.27$ ESR signal with an intensity similar to that of the narrow ESR line.

To explore the origin of the latter ESR signal, both initial Mg (99.9%) and amorphous B (99%) powders were independently measured. No appreciable ESR signal was detected for the Mg powder, while a very sharp resonance line with $g = 2.0037(5)$ and $\Delta H_{pp} \approx 4(1)$ G was found in the B pow-

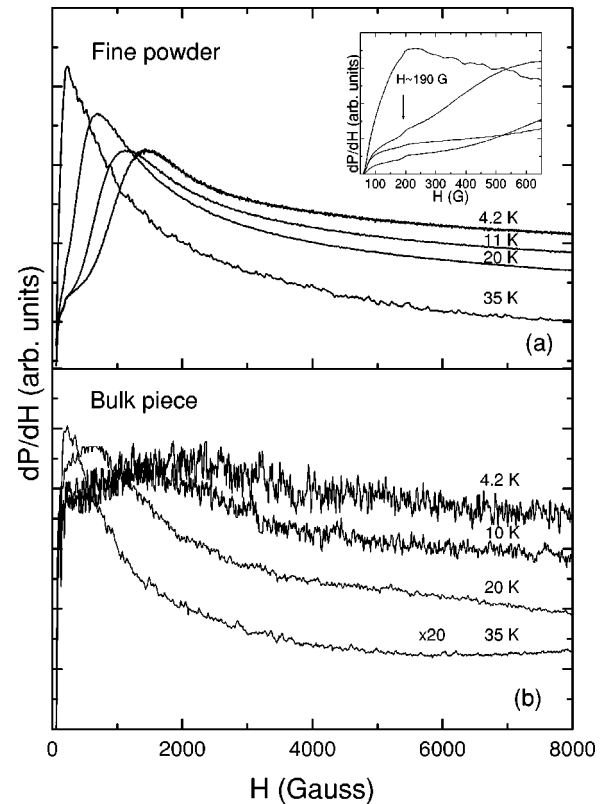


FIG. 2. Temperature dependence of MMMA for (a) a fine powder sample at microwave power of $3.6 \mu\text{W}$ and (b) the bulk specimen at microwave power of 3.6 mW . The inset shows in detail the low-field MMMA, where the weak singularity is depicted by an arrow.

der. The spin concentration in the B powder is $\sim 1.4 \times 10^{18}$ spin/g B, which amounts to about 6.7×10^{17} spin/g MgB_2 , in close agreement with the defect spin concentration estimated for MgB_2 . Relying on the similarity of the g values to the free-electron g factor ($g_e = 2.0023$) and their comparable intensities, a plausible interpretation of these ESR signals might be sought in the presence of oxygen radicals.¹⁴ Such oxygen defects may be formed in the minor boron oxide phases, persistent in both the amorphous B powder and the grain boundaries of the MgB_2 samples.¹⁵ In the latter case, the paramagnetic centers appear to be incorporated into the metallic state, unlike the ESR of copper defects in high- T_c cuprates.

Below T_c a pronounced nonresonant signal due to the magnetically modulated microwave absorption (MMMA), greatly enhanced by the resonant cavity, is detected inhibiting the observation of the CESR signal [Fig. 2(a)]. However, for a specimen, further ground with SnO_2 , the CESR signal was gradually restored at $T < 10$ K. Lorentzian fits of CESR, applying below $T \approx 8$ K, showed a broadening and shift of the line, which at 4.2 K corresponded to $g = 1.998(1)$ and $\Delta H = 68(2)$ G, with respect to the normal state. The CESR intensity was also reduced by approximately 50% from the normal-state value at 40 K. Although CESR is, in principle, anticipated in the mixed state of type-II superconductors due to either normal electron states bound to vortices or quasi-

particle excitations over the gap at finite T ,¹⁶ the diamagnetic CESR shift, caused by screening currents that reduce the local field, is rather small compared to the corresponding shifts reported at higher frequencies for MgB_2 .⁵ Repeated measurements on pure MgB_2 specimens failed to reveal the CESR line in the superconducting state, where the MMMA signal was always dominant. This intriguing behavior can most likely be explained by a small part of the sample that remains in the normal state, probably due to some grain damage or surface degradation.

The MMMA signal exhibits a steep rise at $H < 100$ G followed by a substantially reduced slope up to $H \approx 500$ G, and then rises rapidly up to a broad, though pronounced, maximum, which shifts to lower fields as T decreases [Fig. 2(a)]. The field H_{max} , where the maximum of MMMA occurs, is very close to the peak values H_p determined from isothermal magnetization loops of the corresponding MgB_2 powder samples at 1100, 1000, and 700 G at 5, 10, and 20 K, respectively.⁹ Closer inspection of the low-field MMMA shows a weak but sharp singularity close to $H \approx 200$ G that is smeared out at higher T by the broad peak that shifts to lower fields [inset of Fig. 2(a)]. This behavior is in marked contrast with the narrow, derivativelike MMMA signals observed at much lower fields in high- T_c superconductors due to Josephson junctions caused by weak links or other defects, and the concomitant microwave losses stemming from the very low viscosity of Josephson vortices.^{17,18} The observed MMMA more closely resembles that of conventional metallic superconductors, where viscous flux motion causes microwave dissipation through the response of weakly pinned vortices in the presence of dc and weak modulation fields.^{4,19–21} To explore the MMMA response of MgB_2 further measurements were conducted below T_c on the bulk specimen [Fig. 2(b)]. In this case, the MMMA intensity is greatly reduced, while its field and temperature dependence resemble those of the powder samples. Accordingly, the MMMA signal appears to be mostly akin to the powder state rather than the bulk state of MgB_2 , whose MMMA may arise from loosely connected surface grains in accord with its weak and powder CESR.

The steep rise of MMMA for both powder and bulk specimens at low fields, presumably smaller than the lower critical field ($H < 100$ G $< H_{c1}$), might be caused by a relatively small number of irregularly shaped crystallites with sharp edges and high demagnetizing factors easing fluxon entry and vortex motion, as previously observed for Nb_3Sn granular samples.²⁰ Alternatively, a rather small weak-link contribution may be present, as proposed in recent MMMA studies of MgB_2 pellets that exhibited a similar low-field behavior.^{22,23} The subsequent retardation of the MMMA increasing slope along with the narrow peak at $H \sim 200$ G fall very close to the range where H_{c1} sets in,²⁴ considering that H_{c1} may be spanning an appreciable field range for random powders with significant anisotropy. As the magnetic field is further increased, the system is driven in a mixed state of type-II superconductors, where microwave losses may be caused by the dumped motion of weakly pinned vortices confined by surface barriers in the individual crystallites rather than strong pinning.⁹ Paramagnetic defects, such as those identified by ESR in the MgB_2 crystallites, are not expected to pin efficiently the flux lines due to the relatively large ξ_0 , whereas large-scale defects located at grain boundaries of bulk samples may cause substantial bulk pinning that may also account for the reduced MMMA in the bulk specimen. However, further work is needed to establish the origin of the MMMA response and its precise relation to vortex dynamics in MgB_2 .

In conclusion, a comparative ESR study of powder and bulk specimens of MgB_2 verifies the presence of intense CESR in the normal state, with a relatively high spin-relaxation rate and a Pauli susceptibility of $\chi_s = 2.5(4) \times 10^{-5}$ emu/mole. A paramagnetic center of low concentration, presumably due to oxygen defects stemming from the amorphous B powder, along with traces of Fe^{3+} impurities are also identified. The intense microwave absorption observed below T_c in fine powder samples is in accord with the enhanced microwave losses due to the viscous flux motion in contrast to high- T_c superconductors.

This work was supported by the Greek Secretariat for Research and Technology through the PENED program (99ED186).

¹J. Nagamatsu, N. Nakagawa, T. Muranaka, Y. Zenitani, and J. Akimitsu, *Nature (London)* **410**, 63 (2001).

²C. Buzea and T. Yamashita, *Supercond. Sci. Technol.* **14**, R115 (2001).

³D.C. Larbalestier *et al.*, *Nature (London)* **410**, 186 (2001); D.K. Finnemore, J.E. Ostenson, S.L. Bud'ko, G. Lapertot, and P.C. Canfield, *Phys. Rev. Lett.* **86**, 2420 (2001).

⁴K. W. Blazey, in *Earlier and Recent Aspects of Superconductivity*, edited by J. G. Bednorz and K. A. Muller, Springer Series in Solid State Sciences Vol. 90 (Springer-Verlag, Berlin, 1990), p. 262.

⁵F. Simon, A. Janossy, T. Feher, F. Muranyi, S. Garaj, L. Forro, C. Petrovic, S.L. Bud'ko, G. Lapertot, V.G. Kogan, and P.C. Canfield, *Phys. Rev. Lett.* **87**, 047002 (2001).

⁶S.L. Bud'ko, C. Petrovic, G. Lapertot, C.E. Cunningham, P.C. Canfield, M.-H. Jung, and A.H. Lacerda, *Phys. Rev. B* **63**, 220503 (2001).

⁷S.L. Bud'ko, V.G. Kogan, and P.C. Canfield, *Phys. Rev. B* **64**, 180506(R) (2001).

⁸G. Papavassiliou, M. Pissas, M. Fardis, M. Karayanni, and C. Christides, *Phys. Rev. B* **65**, 012510 (2001).

⁹M. Pissas, E. Moraitakis, D. Stamopoulos, G. Papavassiliou, V. Psycharis, and S. Koutandos, *J. Supercond.* **14**, 615 (2001).

¹⁰J.H. Pifer and R. Magno, *Phys. Rev. B* **3**, 663 (1972).

¹¹G. Feher and A.F. Kip, *Phys. Rev.* **98**, 337 (1955).

¹²M. Godlewski, H. Przybylińska, and J.M. Langer, *Appl. Phys. A: Solids Surf.* **30**, 105 (1983).

¹³J. Kortus, I.I. Mazin, K.D. Belashchenko, V.P. Antropov, and L.L.

- Boyer, Phys. Rev. Lett. **86**, 4656 (2001).
- ¹⁴M. Che, in *Magnetic Resonance in Colloid and Interface Science*, Vol. 6 of *NATO Advanced Study Institute, Series C: Mathematical and Physical Sciences*, edited by J. P. Fraissard and H. A. Resing (Reidel, Dordrecht, 1980), p. 79.
- ¹⁵R.F. Klie, J.C. Idrobo, N.D. Browning, K.A. Regan, N.S. Rogado, and R.J. Cava, Appl. Phys. Lett. **79**, 1837 (2001).
- ¹⁶N.M. Nemes, J.E. Fischer, G. Baumgartner, L. Forro, T. Feher, G. Oszlanyi, F. Simon, and A. Janossy, Phys. Rev. B **61**, 7118 (2000) and references therein.
- ¹⁷B. Nebendahl, C. Kessler, D.-N. Peligrad, and M. Mehring, Physica C **209**, 362 (1993).
- ¹⁸V.V. Srinivasu, B. Thomas, M.S. Hedge, and S.V. Bhat, J. Appl. Phys. **75**, 4131 (1994).
- ¹⁹Yu.N. Shavcko, D.Z. Khusainov, A.A. Romanyukha, and V.V. Ustinov, Solid State Commun. **69**, 611 (1989).
- ²⁰M. Mahel and S. Benacka, Solid State Commun. **83**, 615 (1992).
- ²¹J. Dumas, C. Schlenker, B. Thrane, and A. Neminsky, in *Micro-wave Studies of High Temperature Superconductors*, edited by A. Narlicar, Studies of High Temperature Superconductors Vol. 17 (Nova Science, New York, 1996), p. 1.
- ²²M.K. Bhide, R.M. Kadam, M.D. Sastry, A. Singh, S. Sen, D.K. Aswal, S.K. Gupta, and V.C. Sahni, Supercond. Sci. Technol. **14**, 572 (2001).
- ²³J.P. Joshi, S. Sarangi, A.K. Sood, and S.V. Bhat, cond-mat/0103369 (unpublished).
- ²⁴S.L. Li, H.H. Wen, Z.W. Zhao, Y.M. Ni, Z.A. Ren, G.C. Che, H.P. Yang, Z.Y. Liu, and Z.X. Zhao, Phys. Rev. B **64**, 094522 (2001).